CORE
Metadata, citation and similar papers at core.ac.uk
Provided by Tomsk State University Repository

ISSN 1064-2269, Journal of Communications Technology and Electronics, 2018, Vol. 63, No. 3, pp. 281–284. © Pleiades Publishing, Inc., 2018.
Original Russian Text © A.V. Voitsekhovskii, S.N. Nesmelov, S.M. Dzyadukh, V.V. Vasil'ev, V.S. Varavin, S.A. Dvoretsky, N.N. Mikhailov, M.V. Yakushev, G.Yu. Sidorov, 2016, published in Prikladnaya Fizika, 2016, No. 4, pp. 58–61.

Impact of the Graded-Gap Layer on the Admittance of MIS Structures Based on MBE-Grown n-$Hg_{1-x}Cd_xTe$ (x = 0.22–0.23) with the Al_2O_3 Insulator

A. V. Voitsekhovskii[a], *, S. N. Nesmelov[a], S. M. Dzyadukh[a], V. V. Vasil'ev[b], **, V. S. Varavin[b], S. A. Dvoretsky[a, b], N. N. Mikhailov[b], M. V. Yakushev[b], and G. Yu. Sidorov[b]

[a]*National Research Tomsk State University, Tomsk, 634050 Russia*
[b]*Institute of Semiconductor Physics, Siberian Branch, Russian Academy of Sciences, Novosibirsk, 630090 Russia*
**e-mail: vav43@mail.tsu.ru*
***e-mail: ifp@isp.nsc.ru*
Received June 8, 2016

Abstract—The impact of the presence of the near-surface graded-gap layers with an increased content of CdTe on the admittance of MIS structures based on MBE-grown n-$Hg_{1-x}Cd_xTe$ (x = 0.22–0.23) with the Al_2O_3 insulating coating has been experimentally studied. It has been shown that the structures with a graded-gap layer are characterized by a deeper and wider capacitance dip in the low-frequency capacitance–voltage (CV) characteristic and by higher values of the differential resistance of the space-charge region than the structures without such a layer. It has been found that the main features of the hysteresis of capacitance dependences typical of the graded-gap structures with SiO_2/Si_3N_4 are also characteristic of the MIS structures with the Al_2O_3 insulator. The factors that cause an increase in the CV characteristic hysteresis upon formation of the graded-gap layer in structures with SiO_2/Si_3N_4 or Al_2O_3 are still debatable, although it may be assumed that oxygen plays a certain role in formation of this hysteresis.

Keywords: MIS structure, HgCdTe, aluminum oxide, graded-gap layer, admittance, capacitance–voltage characteristic, hysteresis

DOI: 10.1134/S106422691803021X

INTRODUCTION

Narrow-gap semiconducting solid solution of mercury–cadmium-telluride is widely used in manufacturing of high-sensitivity infrared detectors [1, 2]. The width of the $Hg_{1-x}Cd_xTe$ forbidden gap depends on the content of CdTe, which makes it possible to build detectors for various spectral regions on the basis of this material. One of the main types of detectors based on the narrow-gap semiconducting solid solution of $Hg_{1-x}Cd_xTe$ is formed by matrix diodes for the spectral range of the atmospheric transparency window (8–12 μm), which are made on the basis of $Hg_{1-x}Cd_xTe$ p–n junctions at x = 0.21–0.23 [1–3].

A promising technique for growing HgCdTe is the molecular beam epitaxy (MBE), which makes it possible to grow films with a specified distribution of the composition over the thickness of the epitaxially grown film. This possibility is used to optimize the characteristics of infrared detectors by growing near-surface graded-gap layers with an increased content of CdTe. These layers improve the threshold characteristics of HgCdTe-based infrared detectors owing to minimization of the effect of the surface recombination on the lifetime of photocarriers in the volume of the epitaxial film [3, 4]. The characteristics of HgCdTe-based detectors depend to a large extend on the parameters of the insulating passivating coating and the coating–semiconductor interface [5]; therefore, the analysis of the characteristics of MIS structures based on the MBE-grown heteroepitaxial HgCdTe remains a topical problem.

The possibilities of application of conventional methods for characterization of passivating coatings by means of investigation of the electrophysical characteristics of MIS structures [6] are limited by the features of the MIS structures grown by the MBE of HgCdTe, namely, by the high resistance of the volume of the epitaxial film and also by possible presence of a near-surface varied-gap layer. Experimental investigations of the properties of MIS structures based on MBE-grown HgCdTe with a near-surface graded-gap layer are so far not numerous [7–14]; besides, in these investigations, SiO_2/Si_3N_4 [7–11], anode oxide [7], or CdTe [14] were used as insulators. A promising passivating coating is aluminum oxide Al_2O_3 formed by means of plasma-enhanced atomic-layer deposition

Table 1. Technological parameters of the heterostructures

Structure number	Composition on the surface	Thickness of the upper graded-gap layer, μm	Thickness of the lower graded-gap layer, μm	Composition in the working layer	Thickness of the working layer, μm
1	0.46	0.5	1.0	0.22	6.3
2	0.22	None	1.0	0.22	6.3
3	0.43	0.5	1.3	0.23	7.9
4	0.23	None	1.3	0.23	7.9

Table 2. Electrical parameters of the heterostructures ($T = 77$ K)

Structure number	Concentration of majority carriers, cm^{-3}	Carrier mobility, $cm^2\ V^{-1}\ s^{-1}$	Conductivity, $\Omega^{-1}\ cm^{-1}$	Lifetime, μs
1.2	5.4×10^{14}	34000	3.1	
3.4	3.4×10^{14}	69000	3.9	5.1–7.2

(PE ALD) [15]. This coating can be obtained at near-room temperatures; it also effectively solves the problem of recombination of minority carriers at the interface.

The objective of this study is to investigate experimentally the impact of the presence of the near-surface graded-gap layers with an increased CdTe content on the admittance (complex admittance for a harmonic signal) of MIS structures based on MBE-grown n-$Hg_{1-x}Cd_xTe$ ($x = 0.22$–0.23) with the Al_2O_3 insulating coating.

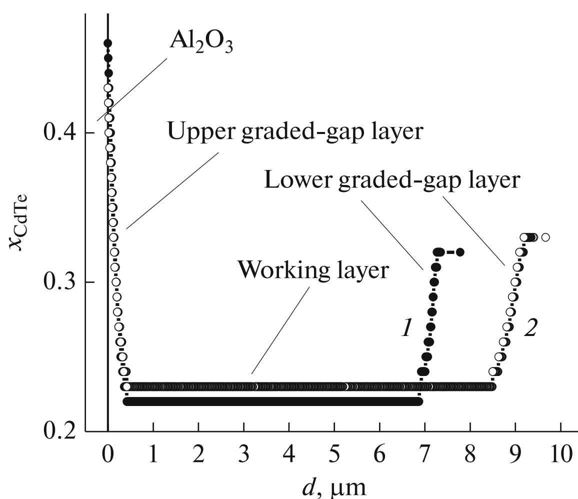

Fig. 1. Relative CdTe content x_{CdTe} versus film thickness d for (curve *1*) structure 1 and (curve *2*) structure 2 based on MBE-grown $Hg_{1-x}Cd_xTe$.

1. TEST SAMPLES AND EXPERIMENTAL TECHNIQUE

The tested heteroepitaxial structures based on n-$Hg_{1-x}Cd_xTe$ ($x = 0.22$–0.23) were grown by the MBE technique on Si(013) substrates at the Institute of Semiconductor Physics, Siberian Branch, Russian Academy of Sciences. During the heterostructure growth process, graded-gap layers with an increased composition (x) were formed on both sides of the working layer. Prior to application of the insulating coating, concentrations of majority carriers, electron mobilities, and admittances were determined for the heterostructures under investigation by the Hall method. The lifetime of minority carriers was determined with the use of a contactless microwave technique. Technological parameters of certain investigated structures are listed in Table 1. Electric parameters of the heterostructures are given in Table 2. In structures 2 and 4, the near-surface graded-gap layer was removed by etching the surface in the Br_2–HBr solution; afterwards, a 70-nm-thick layer of the Al_2O_3 insulator was deposited. In structures 1 and 3, the Al_2O_3 insulator was deposited on top of the graded-gap layer. The distribution of the composition over the film thickness for structures 1 and 3 measured by an automatic ellipsometer in the process of growing is shown in Fig. 1.

The measurements were performed with the use of an automated instrument for the admittance spectroscopy of nanoheterostructures based on a Janis cryostat and an Agilent E4980A immitance meter [8, 9]. In the course of measurements, it was assumed that the voltage variation from negative values to positive corre-

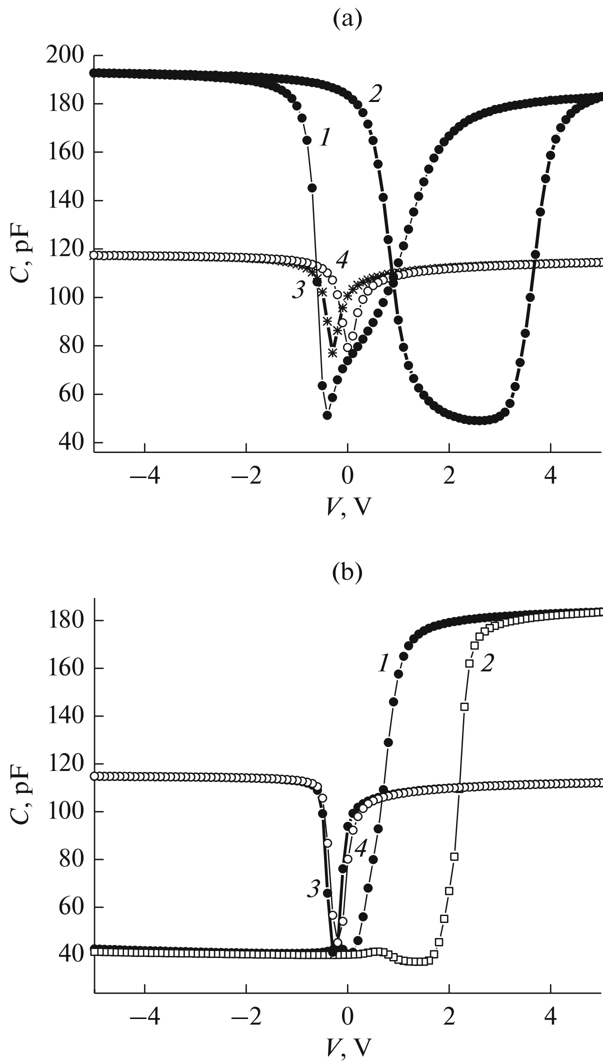

Fig. 2. Capacitance C versus bias voltage V for the MIS structure based on n-$Hg_{0.78}Cd_{0.22}Te$ (structure 1, curves *1, 2*) with and (structure 2, curves *3, 4*) without a graded-gap layer measured at a frequency of (a) 10 kHz and (b) 100 kHz for a temperatures of (a) 77 K and (b) 10 K at the (curves *1, 3*) forward and (curves *2, 4*) reverse sweeping.

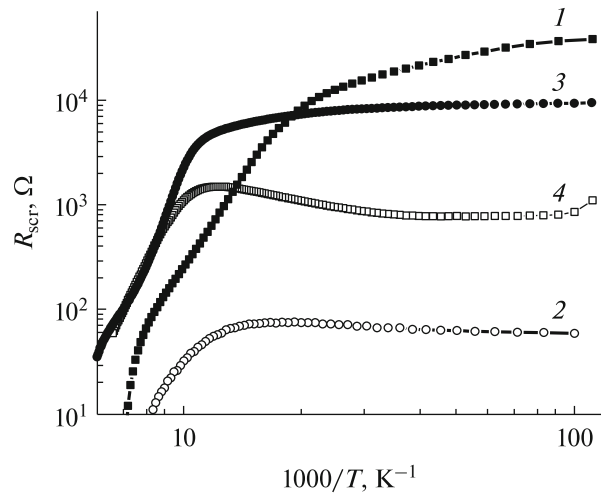

Fig. 3. Differential resistance R_{scr} versus inverse temperature for the MIS structures based on n-$Hg_{1-x}Cd_xTe$ (x = 0.22, structures 1, 2, curves *1, 2*; and x = 0.23, structures 3, 4, curves *3, 4*) (curves *1, 2*) with the graded-gap layer and (curves *3, 4*) without the graded-gap layer measured at a frequency of 100 kHz under strong inversion at the forward sweeping.

sponds to forward sweeping and the voltage variation from positive values to negative corresponds to reverse sweeping.

2. RESULTS AND DISCUSSION

Figure 2 shows capacitance–voltage characteristics of MIS structures 1 and 2 measured at a frequency of 10 kHz for a temperature of 77 K and at a frequency of 100 kHz for a temperature of 10 K, respectively, at the forward and reverse sweeping. It can be seen in Fig. 2a that, for structure 1 with a graded-gap layer, the hysteresis caused by the slow-state trapping of charge carriers in the insulator and at the interface is clearly pronounced [16]. The CV curve hysteresis for structure 2 without a graded-gap layer is relatively small. The depth and width of the dip of the low-frequency CV characteristic of structure 1 with a graded-gap layer is considerably larger than the CV curve of the structure 2 without a graded-gap layer.

At a temperature of 10 K and a frequency of 100 kHz, the CV characteristic of structure 1 with a graded-gap layer assumes the shape of this characteristic at a high frequency whereas the shape of the CV curve of structure 2 without a grade-gap layer is similar to that of the low-frequency characteristic. For structure 2 without a graded-gap layer taken at a temperature of 10 K, a decrease in the capacitance values is observed at the minimum of the low-frequency CV curve with an increase in frequency, which is caused by a decrease in the contribution of the surface-state recharge capacitance to the total capacitance of the structure. For the structures with graded-gap layers, no frequency dispersion is observed since, at temperatures of 10–77 K, the CV characteristic has the high-frequency shape as to the surface-state recharging time [17, 18].

The CV curves of MIS structures 3 and 4 measured at a frequency of 10 kHz for a temperature 77 K at the forward and reverse sweeping have shown that structure 3 with a graded-gap layer exhibits a considerably larger hysteresis, whereas the low-frequency CV characteristics of structure 3 have a deeper and wider capacitance dip as compared to structure 4 without a graded-gap layer.

Figure 3 shows the temperature dependences of the differential resistance of the space charge region (R_{scr}) in the strong inversion mode for structures 1–4, which

were determined at a frequency of 100 kHz for the forward sweeping. It follows from the figure that R_{scr} is higher for structures 1 and 3 with graded-gap layers.

The high-temperature drop of R_{scr} is due to the diffusion of minority carriers from the bulk to the surface. Higher values of R_{scr} in the structures based on MBE-grown n-$Hg_{1-x}Cd_xTe$ (x = 0.21–0.23) with a graded-gap layer are caused by suppression of the tunneling through deep levels [8]. It is probable that, for structures with a graded-gap layer, R_{scr} is limited by the Shockley–Read generation processes, although simulation with the use of the expressions from [19] results in dependence $R_{scr}(T)$ that is sharper than the experimental curve.

CONCLUSIONS

In this study, the effect of the presence of the near-surface graded-gap layers with an increased CdTe content on the admittance of the MIS structures based on MBE-grown n-$Hg_{1-x}Cd_xTe$ (x = 0.22–0.23) with the Al_2O_3 insulator has been investigated. As expected, a larger depth and width of the capacitance dip on the low-frequency CV characteristic is observed for structures with the graded-gap layer. A similar result was earlier obtained for MIS structures based on the MBE-grown n-$Hg_{1-x}Cd_xTe$ (x = 0.21–0.23) with the double-layer SiO_2/Si_3N_4 insulator [8, 9]. The larger depth and width of the capacitance dip in the low-frequency CV curve for structures with the graded-gap layer is due to the fact that the intrinsic concentration in graded-gap structures is lower at the interface, which results in a change in the voltage dependence of the surface potential [20]. The CV curve hysteresis in MIS structures based on the n-$Hg_{1-x}Cd_xTe$ (x = 0.21–0.23) with SiO_2/Si_3N_4 is determined by the recharging of slow states located near the interface [16].

All main features of the hysteresis determined for structures with SiO_2/Si_3N_4 are also observed in the MIS structures with Al_2O_3. A slight difference is that the values of the capacitance at the minimum of the low-frequency CV characteristic for structures with Al_2O_3 may be nearly the same at both forward and reverse sweeps of voltage (structure 1). This may be due to the fact that, in the transition layer of structure 1, the concentration of impurity defects recharging under the action of the voltage is low.

The factors that cause an increase in the CV curve hysteresis when the graded-gap layer is formed in structures with SiO_2/Si_3N_4 or Al_2O_3 are still debatable, although it may be assumed that oxygen plays a certain role in formation of the hysteresis (a similar increase in the CV curve hysteresis was observed for the structures with anode oxide, but it was very small for the structures with CdTe grown in situ [14]). Higher values of R_{scr} in the structures based on MBE-grown n-$Hg_{1-x}Cd_xTe$ (x = 0.21–0.23) with a graded-gap layer are due to suppression of tunneling through deep levels [8].

ACKNOWLEDGMENTS

This study was supported by the Russian Foundation for Basic Research and the Administration of the Tomsk Region, project no. 16-42-700759.

REFERENCES

1. A. Rogalski, *Infrared Detectors* (CRC Press, Taylor & Francis Group, New York, 2011).
2. P. Capper and J. Garland, *Mercury Cadmium Telluride: Growth, Properties and Applications* (Wiley, Chichester, 2011).
3. V. N. Ovsyuk, G. L. Kuryshev, and Yu. G. Sidorov, *Focal Plane Arrays of Infrared Range* (Nauka, Novosibirsk, 2001) [in Russian].
4. Yu. G. Sidorov, S. A. Dvoretski, V. S. Varavin, N. N. Mikhalov, M. V. Yakushev, and I. V. Sabinina, Semiconductors **35**, 1045 (2001).
5. O. P. Agnihorti, C. A. Musca, and L. Faraone, Semicond. Sci. Tech. **13**, 839 (1998).
6. E. H. Nicollian and J. R. Brews, *MOS (Metal Oxide Semiconductor) Physics and Technology* (Wiley-Interscience, New York, 2002).
7. A. V. Voitsekhovskii, S. N. Nesmelov, and A. P. Kokhanenko, Russian Phys. J. **48** (2), 143–147 (2005).
8. A. V. Voitsekhovskii, S. N. Nesmelov, and S. M. Dzyadukh, et al., Russian Phys. J. **57**, 536 (2014).
9. A. V. Voitsekhovskii, S. N. Nesmelov, and S. M. Dzyadukh, Opto-Electronics Rev. **22** (4), 236 (2014).
10. A. V. Voitsekhovskii, S. N. Nesmelov, S. M. Dzyadukh, et al., Infrared Phys. Technol. **71**, 236 (2015).
11. V. N. Ovsyuk and A. V. Yartsev, Proc. SPIE **6636**, 663617 (2007).
12. V. V. Vasil'ev and Yu. P. Mashukov, Semiconductors **41** (1), 37 (2007).
13. D. I. Gorn, S. N. Nesmelov, A. V. Voitsekhovskii, and A. P. Kokhanenko, Izv. Vyssh. Uchebn. Zaved., Fiz. **51** (9-3), 134 (2008).
14. A. V. Voitsekhovskii, S. N. Nesmelov, S. M. Dzyadukh, V. S. Varavin, S. A. Dvoretsky, N. N. Mikhailov, Yu. G. Sidorov, and M. V. Yakushev, Opto-Electron. Rev. **18** (3), 263 (2010).
15. R. Fu and J. Pattison, Opt. Eng. **51**, 104003-1 (2012).
16. A. V. Voitsekhovskii, S. N. Nesmelov, and S. M. Dzyadukh, Russian Phys. J. **58**, 540 (2015).
17. A. V. Voitsekhovskii, S. N. Nesmelov, and S. M. Dzyadukh, J. Electron. Mater. **45**, 881 (2016).
18. A. V. Voitsekhovskii, S. N. Nesmelov, and S. M. Dzyadukh, Russian Phys. J. **59**, 284–294 (2016).
19. W. He and Z. Celik-Butler, Solid-State Electron. **39** (1), 127 (1996).
20. A. V. Voitsekhovskii, S. N. Nesmelov, S. M. Dzyadukh, et al., Priklad. Fiz., No. 5, 80 (2011).

Translated by I. Nikishin